Fresenius J Anal Chem (2000) 368 : 37–44

SPECIAL ISSUE PAPER

Davide Bleiner · Kathrin Hametner · Detlef Günther

Optimization of a laser ablation-inductively coupled plasma "time of flight" mass spectrometry system for short transient signal acquisition

Received: 6 March 2000 / Revised: 11 May 2000 / Accepted: 14 May 2000

Abstract Simultaneous ion sampling and sequential detection offered by inductively coupled plasma 'time of flight' mass spectrometry *(ICP-TOFMS)* provides advantages for the analysis of short transient concentration-variable signals as produced in laser ablation. In order to investigate the capabilities of ICP-TOFMS in combination with an excimer laser ablation system, ablation studies on reference materials and geological samples were carried out. Various ICP-TOFMS parameters were optimized for laser-induced aerosols. Transverse rejection ion pulse was used to extend the dynamic range in concentration. A reduced volume ablation cell was designed and used in order to increase the sample density in the ICP. Results for 63 simultaneously measured isotopes (SRM 610 from NIST) lead to limits of detection in the 1–100 μg/g range for a 80 μm crater diameter (10 Hz, 1.2 mJ pulse energy). The reproducibility of signal ratios was determined to be better than 2% RSD for transient signals using 102 ms integration time. These optimized parameters were then used for the analysis of tin-rich fluid inclusions. Preliminary results of multielement analysis and isotopic ratio determinations on individual fluid inclusions (63 isotopes, 102 ms integration time) demonstrate the capabilities of ICP-TOFMS in combination with laser ablation.

Introduction

ICP-TOFMS opens a new way in multielemental analysis and the acquisition of fast transient signals [1, 2]. The acquisition of 20,000 spectra per second and a fast data readout time allow the introduction and detection of very short concentration-variable transient signals of samples of small volume, which is interesting in flow injection analysis (FIA), electrothermal vaporization (ETV), direct sample insertion (DSI) and in laser ablation (LA).

D. Bleiner · K. Hametner · D. Günther (✉)
Laboratorium für Anorganische Chemie, ETH Zürich,
Universitätsstrasse 6, CH–8092 Zürich, Switzerland

Studies of isotope ratio stability [3] using ICP-TOFMS showed similar precision to that established for single-collector sector field ICP-MS operated at low resolution. However, in ICP-TOFMS the number of isotopes measured has no influence on the precision and an extended element menu can be selected. As reported [4], sensitivity in the middle to high mass range is approx. 2000 cps/(ng g^{-1}), which is at least one order of magnitude less than ICP-QMS, resulting in limits of detection (LOD) of 1–50 pg/g for solution nebulization. The linear dynamic range of the instrument used is approx. 6 orders of magnitude. This limited linear dynamic range in concentration has a strong influence on the flexibility in solid sampling, where major, minor and trace elements from a single ablation spot are of interest.

The aim of this study was to investigate optimum operating conditions for laser-induced aerosol introduced into an ICP-TOFMS. The initial system optimization was carried out using solution nebulization under different conditions and the analytical performance was determined. Duration of opening of the ion-sampling gate (modulation pulse width) was extended in order to enhance sensitivity; transverse rejection ion pulse (T.R.I.P.) was tested as a possible tool to extend the linear dynamic range in concentration. Laser ablation-ICP-MS is the preferred technique for multielemental analysis of fluid inclusions. To test the potential of the TOF mass analyzer in short transient concentration-variable signal detection, natural fluid inclusions from previous studies [5, 6] were analyzed. Fluid inclusions are multielemental, multiphase samples of limited quantity, which represent relics of magmatic fluids entrapped in a growing host crystal and contain useful information about the original chemical features of ore-bearing fluids. Therefore, the identification and quantification of as many elements as possible in such samples is of great interest in ore-geochemistry.

Experimental

The commercially available axial geometry ICP-TOFMS "*Renaissance*" (LECO Corp., St. Joseph, MI, USA) was used for the mea-

Table 1 Operating parameters of the inductively coupled plasma – time-of-flight-mass spectrometer (Renaissance, LECO Corp. USA)

	Solution nebulization		Laser ablation
	Meinhard	MCN 6000	ArF* 193 nm
ICP			
Plasma flow (L/min)	14	14	13 to 14
Carrier flow (L/min)	0.85	1.00	0.97 to 1.78
Auxiliary flow (L/min)	0.71	1.09	0.98 to 1.27
Power (Watt)	1150	970	1000 to 1100
Torch X pos. (mm)	1.9	1.9	2.0
Torch Y pos. (mm)	–2.0	–2.1	–2.3
Torch Z pos. (mm)	13.0	9.7	11.9 to 15.5
MS			
Ion lens 1 (V)	–518	–750	–510 to –700
Ion lens 2 (V)	–200	–140	–170 to –200
Modulation negative (V)	–103	–100	–100 to –103
Repeller pulse (V)	1000	1000	1000
Repeller bias (V)	0	0	0
Flight tube (V)	–1496	–1500	–1500
Einzel lens 1 (V)	–1444	–1420	–1422 to –1440
Y-steering (V)	–1600	–1620	–1600 to –1620
Einzel lens 2 (V)	–810	–900	–810 to –910
X-steering (V)	–1491	–1490	–1486 to 1496
Reflectron low (V)	195	200	196 to 200
Reflectron high (V)	1555	1560	1554 to 1566

surements in combination with solution nebulization and laser ablation sample introduction systems. RF generator frequency of 40.86 MHz with forward power of approx. 1100 W (depending on the optimization, Table 1) was used. The spectral frequency of 20 kHz allows a single full mass spectrum scan in 50 µs. The resolution of the system is variable over the mass range, and a value of 450–500 at 10% of peak height can be observed. More detailed information is provided in the literature [4].

Solution nebulization experiments were carried out using both a Meinhard concentric nebulizer (type C, solution uptake 2 mL/min) with Wu-Hieftje spray chamber and a micro concentric nebulizer (MCN 6000 Cetac Technologies, Omaha, USA) with desolvating unit (sweep gas flow at 4.46 L/min, solution uptake 60 µL/min).

The ICP-TOFMS was coupled to the commercially available *GeoLas* laser ablation system (MicroLas, Göttingen, Germany), that has been described elsewhere [7]. The laser microprobe is an excimer ArF* 193 nm laser (Compex110I, Lambda Physik, Göttingen, Germany). The system was used under standard operating conditions (180–200 mJ output energy, 10 Hz repetition rate, 20–120 µm spot size), which results in a fluence between 25 and 30 J/cm^2. Helium was flushed as carrier gas through the cell. Ablation experiments were carried out in a 21 cm^3 cylindrical cell and in a newly developed 1.5 cm^3 ablation cell. The latter permits to allocate 8 samples at the same time, similarly as in a wider cylindrical cell. The samples are separated from each other in individual slots to minimize memory effects on the sample surface from previous ablations. The design of the cell is based on a rotating round central sample holder and each sample can be moved into the ablation space by rotating the sample holder plate, like a barrel of a revolver ("gun-barrel" ablation cell). The transfer tube between the ablation cell and the ICPMS was approx. 1 m long (i.d. 4 mm). The gas inlet tube was connected to the cell using a 0.5 mm i.d. nozzle. Operating parameters of the ICP-TOFMS system are summarized in Table 1.

Samples. The optimization procedure was carried out on multielement standard solutions prepared from single element stock solutions (Merck, Darmstadt, Germany). SRM NIST 610 was used for the optimization of the ablation process and for quantification of fluid inclusions, as described in [6].

Quartz-hosted pseudo-secondary fluid inclusions from the Yankee Lode of the Mole Granite (New South Wales, Australia), described extensively in [5], were analyzed. Three sets (jy07, no02 and dc14) of inclusions of a few tens of µm were ablated using the cascade sampling procedure described in [6].

Results and discussion

Ion optics adjustment. The complete set of ion optical elements was studied scanning the complete voltage range and collecting the signals using a multielemental standard solution of 10 ng/g (5 repetitions, total measurement time 10 s each replicate). Each individual parameter was investigated keeping the others at the pre-optimized conditions. Figure 1 shows normalized signal intensity in the low mass region (^{63}Cu), in the middle mass region (^{133}Cs) and in the high mass region (^{209}Bi) as a function of lens voltage. Ion lens 1 is the extraction lens and together with ion lens 2 it is positioned before the modulation/acceleration unit, whereas both Einzel lenses as well as X/Y-steering plates influence the accelerated ion beam. For ion lens 1 a top plateau was reached at a lens voltage more negative than –700 V. The ion lens 2 shows two maxima, which are at –160 V and at –850 V. Einzel lens 1 shows a maximum intensity for all masses between –1200 and –1600 V and sharp peaks (evident for Cu and partly for Cs) with a strong mass dependency at lower lens bias. Therefore, the instrument was operated around –1400 V. The X/Y-steering plates show a Gaussian behavior. The optimization carried out for solution nebulization with Meinhard concentric nebulizer was also applied for laser ablation. The operating conditions

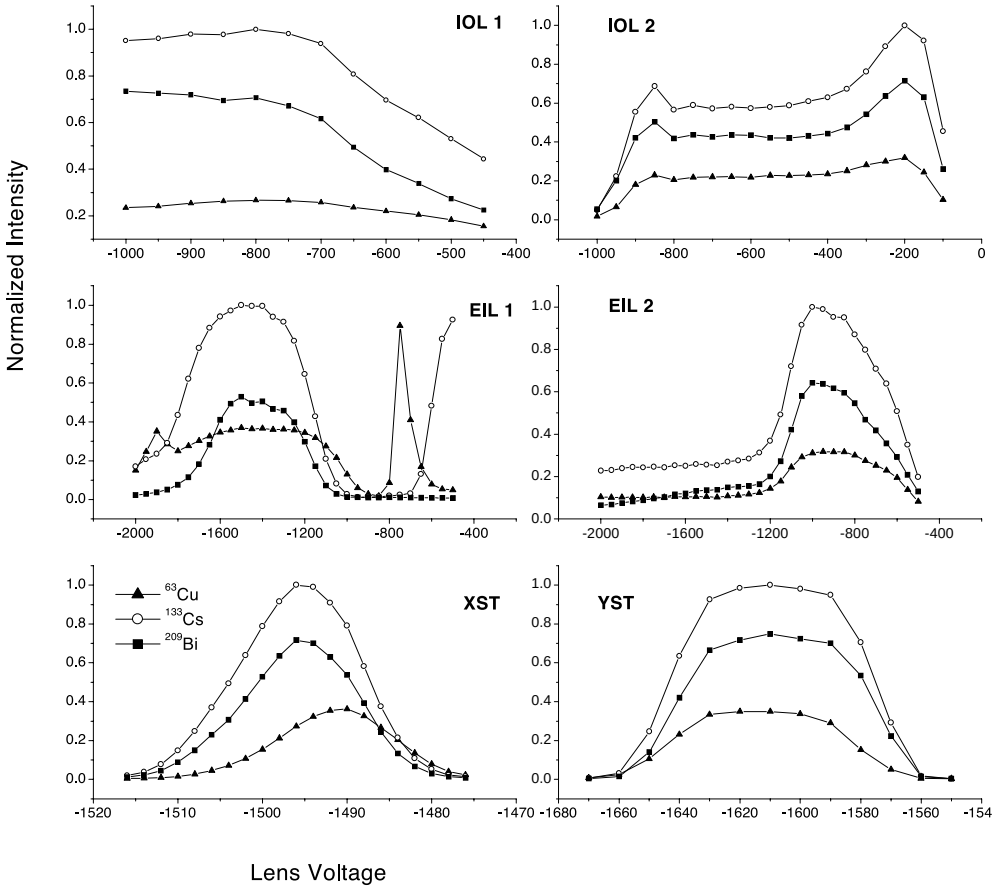

Fig. 1 Normalized signal intensity as a function of lens voltage applied for the ion-optics

summarized in Table 1 show that the ion optics settings were independent of the type of sample introduction (wet or dry aerosols). It should be pointed out that the values summarized in this table were developed for multielemental analysis and reduced oxide formation.

Extension of modulation pulse width. The duration of the opening of the ion sampling gate determines the amount of ions collected per single analytical cycle. Increasing the number of ions per cycle can enhance sensitivity, which is particularly important when dealing with short transient signals of trace/ultratrace elements of very low sample amount. However, a longer sampling duration (*modulation pulse width, MPW*) reduces the effective mass detection duration (*modulation pulse delay, MPD*), since the sum of the two parameters is constant (MPW + MPD = 50 μs, at 20,000 Hz spectral frequency). In axial geometry ICP-TOFMS the source cannot be refilled until the whole ion packet has reached the detector. In fact, one ion packet must remain separated from the next one and sufficient time must be provided to the heaviest (slowest) ion to reach the end of the flight path. The default MPW of 4.89 μs results in a MPD interval of 45.11 μs. This interval can separate ions within a mass range of approx. 345 u (heaviest allowed mass) calculated by the *m/z – flight time* calibration. In order to increase the sensitivity, the MPW was stepwise increased from 4.89 μs (345 u) to 7.28 μs (300 u). Further extension of MPW above 7.28 μs was considered dangerous due to the presence of UO^+ (m/z 254) and UOO^+ (m/z 270), which were detected for liquid sample introduction and for laser ablation. In addition, mass resolution for longer MPW would degrade due to the generation of a less spatially defined ion packet in the source. However, variation of the mass resolution (450–500 as measured at 10% of peak height) was not observed for MPW between 4.89 μs and 7.28 μs. The results for solution nebulization and dry aerosol (laser ablation) measurements are summarized in Fig. 2. The curves for solution nebulization sample introduction show no significant variation (three selected isotopes). The introduction of laser-induced aerosols led to a significant mass-dependent increase in sensitivity (optimum at 5.93 μs). A more significant signal variation for the low mass than for the high mass region was observed. The increase in sensitivity was a factor of 1.5–2.5 depending on the isotope. A possible explanation for the decrease in sensitivity at longer sampling time for dry aerosol might be a too high ion current density producing ion defocusing. In fact, longer MPW might lead to an overfilling of the sampling stage and a stronger space charge is likely.

Transverse rejection ion pulse for wider linear range. Transverse rejection ion pulse (T.R.I.P.) has been described in the literature [4]. This allows a selective removal of in-

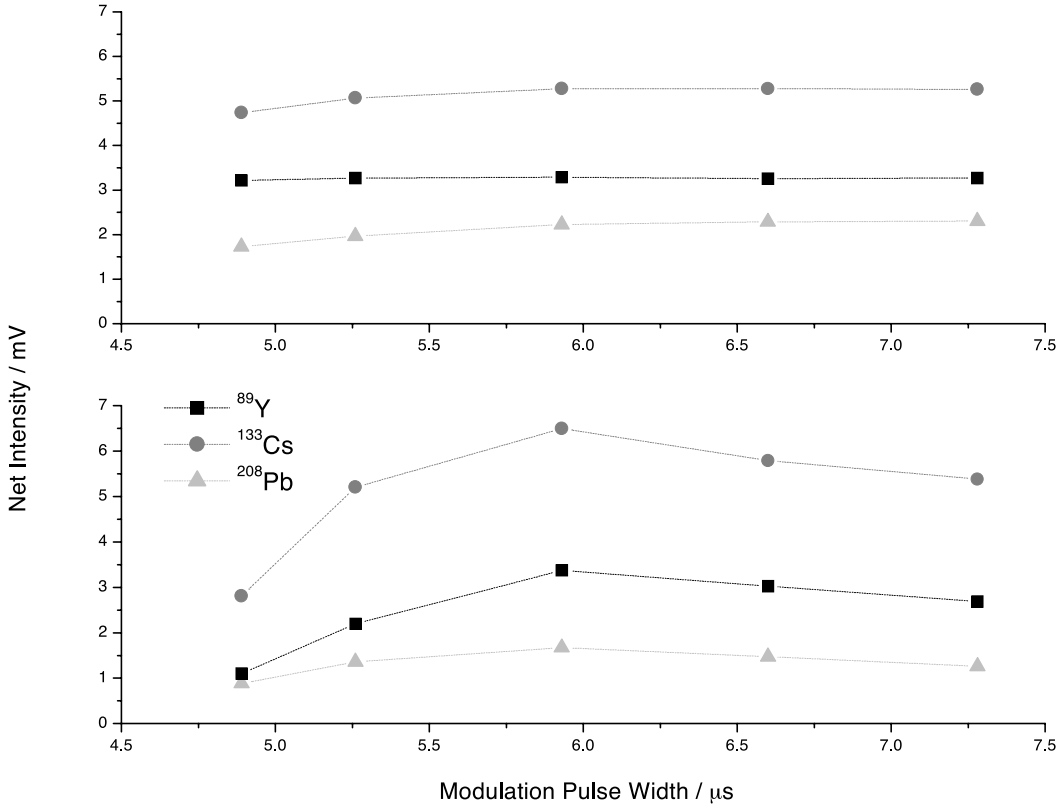

Fig. 2 Signal intensity as a function of modulation pulse width for solution nebulization (*top*) and laser ablation (*bottom*)

terfering species like Ar^+, Ar_2^+, O^+ from the ion beam and was mainly implemented to avoide detector overload. The parameters controlling the ion deflection are the start of the pulse and its duration (or width) and in Table 2 the implemented T.R.I.P. are summarized. In order to extend the linear dynamic range of some high-sensitivity isotopes (e.g. sodium as one of the major elements in fluid inclusions), ion deflection functionality was investigated using different concentration ranges for calibration (within the gain switch limitations). Three calibration curves for different deflected amounts of Na and U (examples for low and high mass region isotopes, see Table 2) from the ion beam were tested using nine standard solutions (Na and U) in a concentration range from 1 to 5000 ng/g (Fig. 3). The linearity of all sodium calibration curves (0.999) indicates the possibility of quantitative removal of matrix ions. In the present experiments half an order of magnitude extension of the linear dynamic range was reached. The same experiments carried out for ^{238}U showed slightly lower linear correlation (0.993). The extension of the linear dynamic range was 1.5 orders of magnitude. The observed mass-dependent variation of the peak shape can explain the difference in the orders of magnitude gained for Na and U and their differences in linearity.

Table 2 Detailed start time and duration for the applied transverse rejection ion pulses to selectively remove matrix ions, Na and U

Deflection	Start/µs	Width/µs
Oxygen-16	0.972	0.14
Argon-36	1.452	0.03
Argon-40	1.534	0.15
Argon dimer-80	2.078	0.03
Sodium-23	1.162	0.03 and 0.05
Uranium-238	3.448	0.050

Optimization of the source conditions. Plasma source conditions (forward RF power, gas flows, torchbox position) for different sample introduction systems and for different ablation cells were optimized for high sensitivity, low background, low oxide formation and low doubly charged ions. CeO^+/Ce^+ was reported [4, 8] with a value of 24.7% for the same type of instrument. Different optimization procedures led to similar oxide formation together with sensitivity of 6 Mio cps/ng g^{-1} (middle mass region). The LOD in Fig. 4, derived from compromised values for low oxide formation and multielement analysis, are very similar for both types of nebulizers. However, major differences were obtained in the oxide formation with 2.2% CeO^+/Ce^+ using the MCN 6000 and 7.0% CeO^+/Ce^+ using the Meinhard nebulizer. The reproducibility of the measurements was in the range of 1% for an integration time of 10 s and 5 repetitions. Further changes of the sample cone geometry and a reduction of the pressure in the expansion chamber using an additional rotary pump showed no significant improvement in sensitivity or reduction of oxide formation.

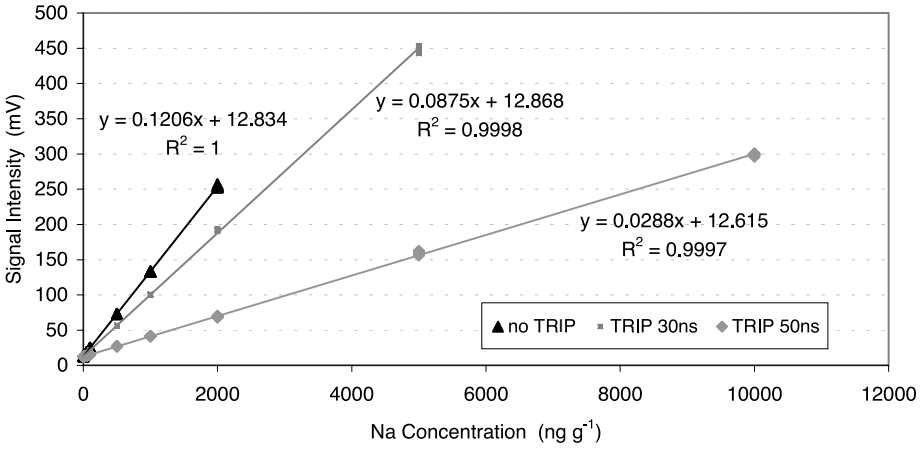

Fig. 3 Transverse rejection ion pulse used to extend the linear range of sodium. Using standard solution in a wide concentration range and partially rejecting a reproducible amount of sodium the slope of the calibration curve decreases, which can be used to extend the linear dynamic range in concentration

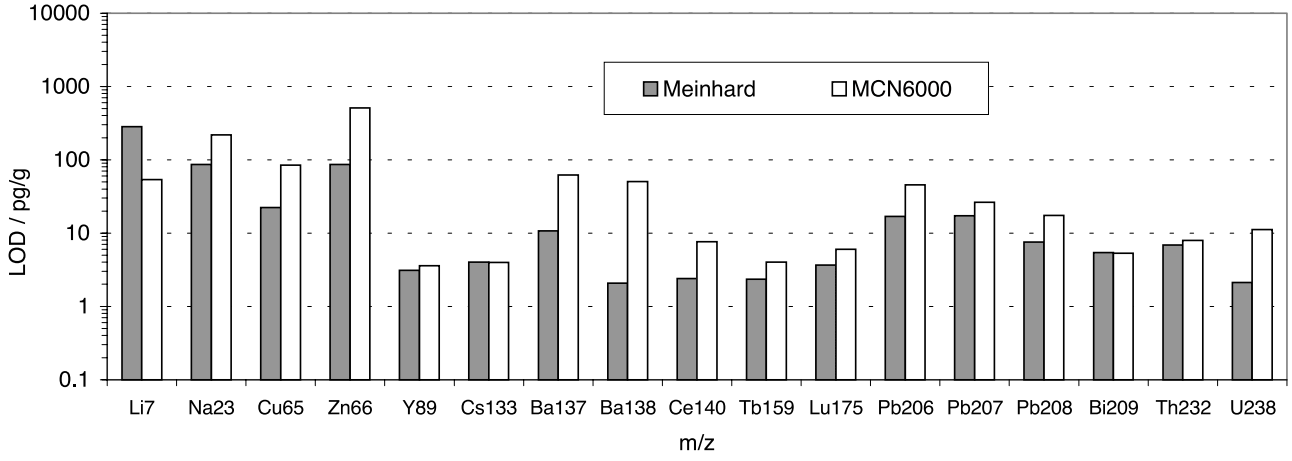

Fig. 4 Limits of detection as derived from solution nebulization using a Meinhard concentric nebulizer and the MCN 6000 (Cetac Technologies Inc.)

Integration time. The influence of integration time on isotopic ratio precision was tested in transient mode (30 s signal acquisition) to evaluate the optimum compromise between high time resolution signal recording as needed for short concentration variable laser ablation and best isotope ratio precision. The relative standard deviations for eight isotope pairs in dependence on the integration time measured using 100 ng/g standard solutions are summarized in Table 3. The precision can be improved using longer integration time. However, for the application of laser ablation analysis on fluid inclusions an extension of the measurement time leads to significant loss of information during the sampling. Therefore, all further experiments were carried out using 102 ms as integration time.

Optimization of the laser ablation system. The dry sample introduction into the ICP-TOFMS was optimized according to the information derived from the solution nebulization experiments. The limits of detection of the system LA-ICP-TOFMS for a 10 Hz repetition rate, 2.8 mJ pulse energy at 80 µm pit size are summarized in Fig. 5. Most of the LOD were determined to be below 100 µg/g (21 cm^3 cylindrical cell). Due to the simultaneous sampling of the

Table 3 Influence of integration time on isotope ratio precision of the measurement. The signal was acquired in transient mode for 30 s from 100 ng/g standard solution

	12 ms	51 ms	102 ms	357 ms	510 ms	714 ms	1007 ms
63/65 Cu	6.1%	3.2%	2.2%	1.2%	1.0%	0.8%	0.8%
86/88 Sr	5.5%	2.8%	2.0%	1.0%	0.9%	0.7%	0.6%
107/109 Ag	3.9%	1.9%	1.4%	0.7%	0.5%	0.5%	0.4%
135/138 Ba	6.1%	3.1%	2.2%	1.3%	1.1%	1.0%	0.6%
177/180 Hf	4.9%	2.5%	1.6%	0.9%	0.8%	0.6%	0.6%
178/180 Hf	4.2%	2.2%	1.5%	0.8%	0.6%	0.5%	0.5%
206/208 Pb	4.0%	1.9%	1.4%	0.8%	0.6%	0.5%	0.5%
207/208 Pb	4.1%	2.1%	1.5%	0.8%	0.7%	0.7%	0.5%

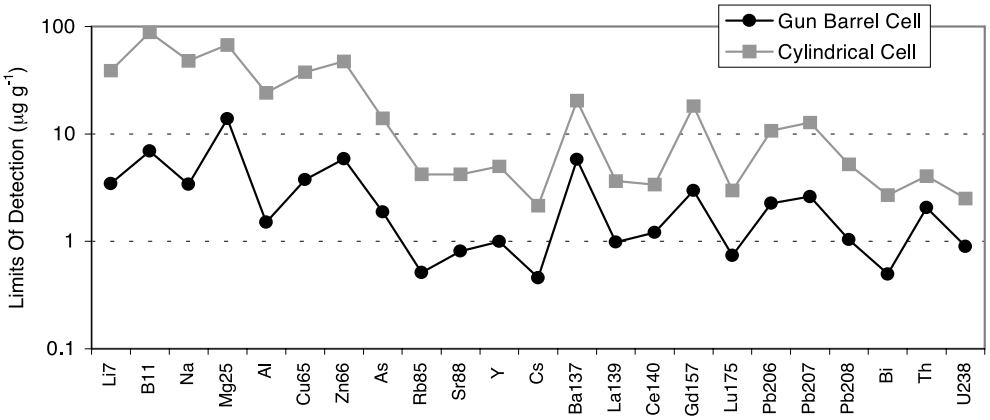

Fig. 5 Limits of detection from the ablation of NIST 610 standard glass with 80 µm spot size (10 Hz repetition rate and 2.8 mJ pulse energy) using the cylindrical 21-cm^3 ablation cell and the newly designed 1.5-cm^3 "gun-barrel" cell

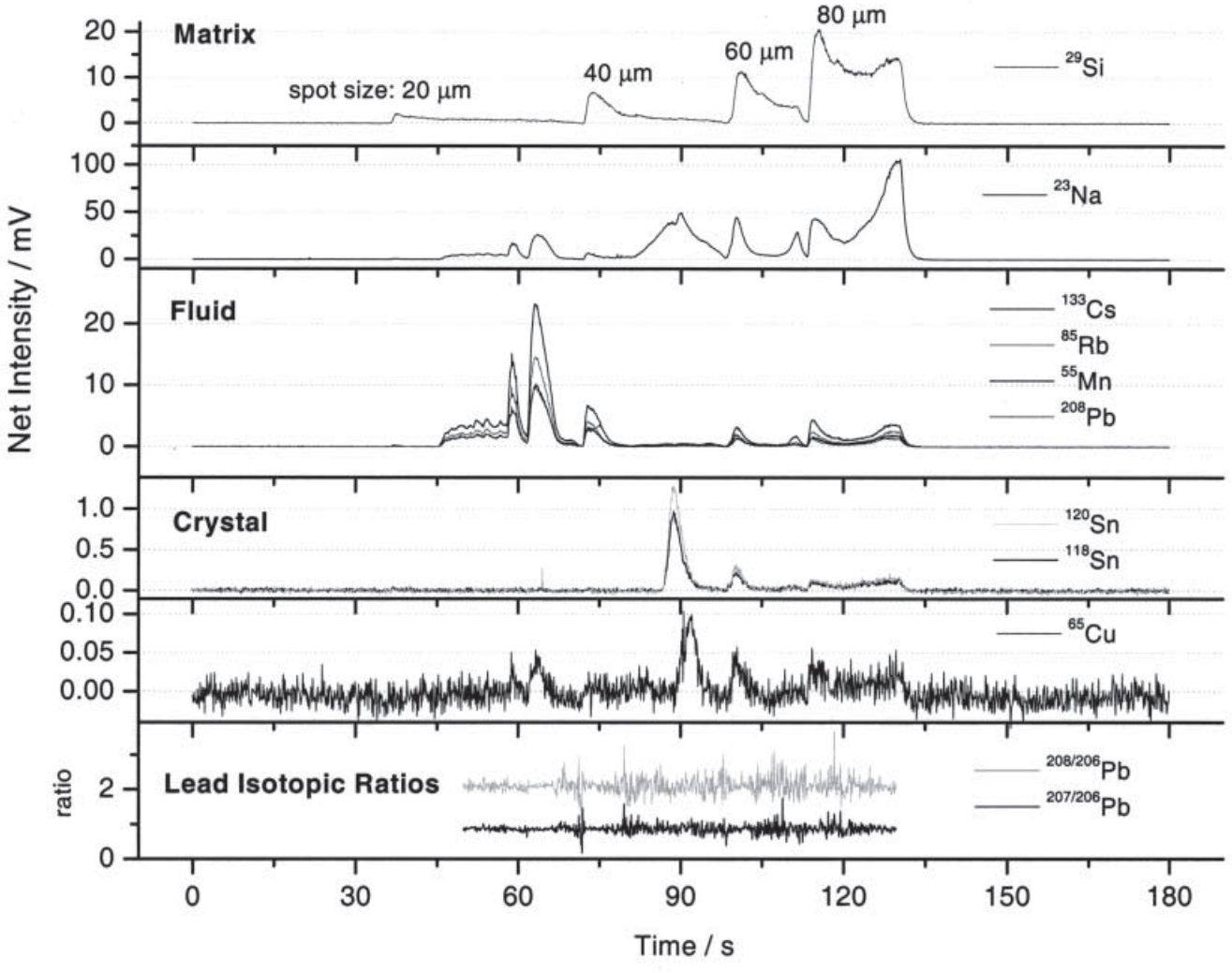

Fig. 6 Cascade ablation of fluid inclusion in quartz (Mole Granite, New South Wales, Australia). The first 34 s of the signal show the measured background (gas blank). After 34 s the laser was started, which can be seen on the quartz matrix signal (Si). At 45 s the inclusion is opened and the signal of the elements contained in the fluid phase appears (e.g. Mn, Rb, Cs, Pb). Finally, the crater diameter is enlarged to empty the inclusion and small signals of the daughter crystal were detected (e.g. Cu, Sn). The lead isotopic ratios of the entire transient (shown at the bottom) indicate a different sampling procedure for precise isotope ratio determination

ions, the sample density in the plasma was increased by ablating the samples in a volume-reduced ablation cell ("gun-barrel"), see Fig. 5. However, the 8–10 times improved LOD can be also related to a more efficient sample transport. Further studies on the ablation cells are in progress to validate these observations.

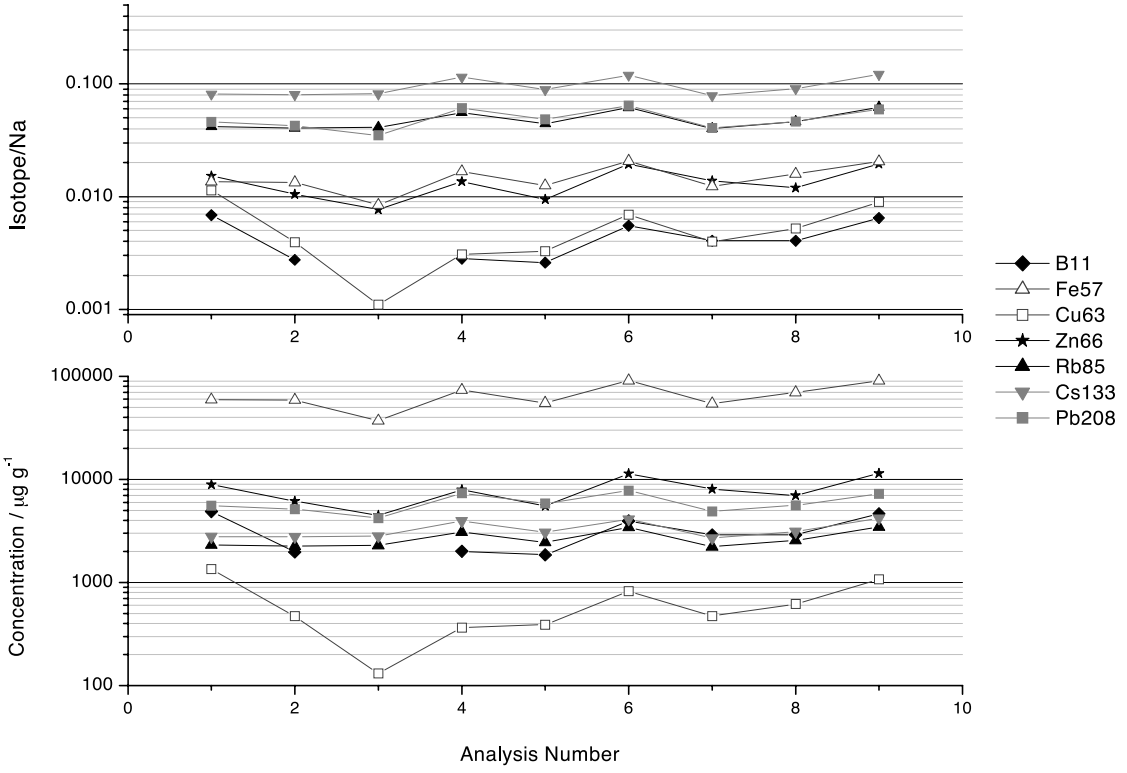

Fig. 7 Reproducibility of elemental ratios (normalized to sodium) for selected isotopes and their corresponding concentrations for a set of nine fluid inclusions

Fluid inclusion analysis using LA-ICP-TOFMS. The optimized system was used to analyze single multiphase fluid inclusions and thus evaluate the capabilities of this simultaneous detection system for such short concentration-variable transient signals. The quartz-hosted inclusions were drilled out using different pit sizes. An integration time of 102 ms was selected and 63 isotopes were measured. Fast drilling through the matrix into the fluid inclusion leads to increased sample density in the plasma and provides improved LOD and better precision. However, to avoid undesired splashing during the opening of the inclusions, the

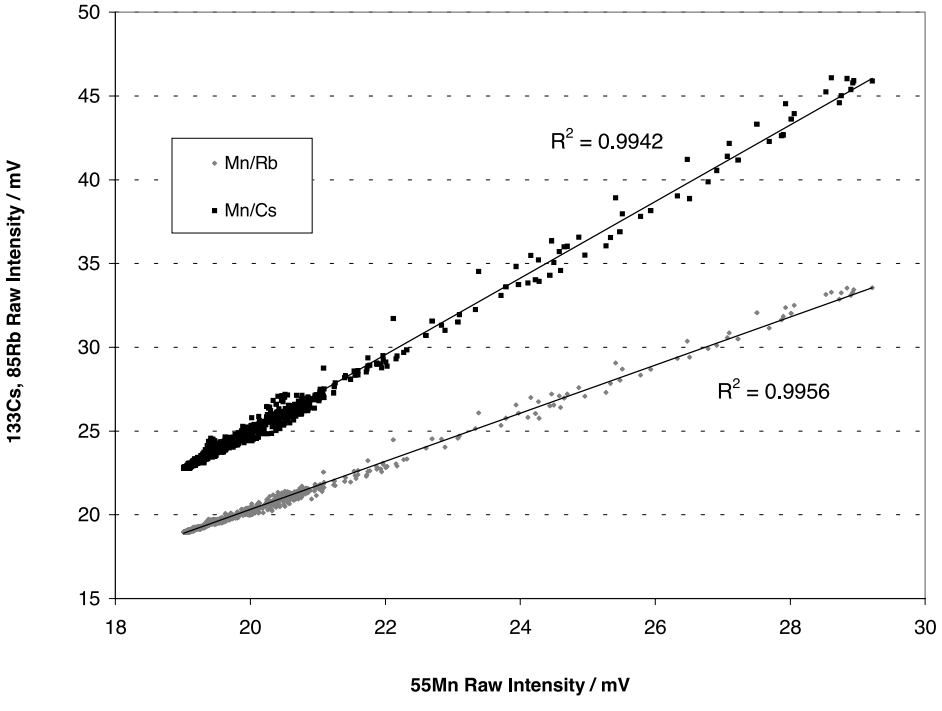

Fig. 8 Inter-elemental correlation. Between elements occurring in the same phase the linear fit is extremely good

Table 4 RSD of lead isotopic ratios determined in a set of nine fluid inclusions, ablated in the "gun-barrel" cell. Improved precision was obtained for major-peak ratios (see also Fig. 6)

	Full signal ratios		Major peak ratios	
	207/206 Pb	208/206 Pb	207/206 Pb	208/206 Pb
Dc14a09	21.3% (n = 128)	17.9%	5.7% (n = 31)	4.7%
Dc14a10	15.5% (n = 137)	11.4%	5.2% (n = 29)	4.3%
Dc14a11	9.9% (n = 140)	8.0%	7.0% (n = 15)	3.3%
Dc14a12	15.8% (n = 116)	12.7%	8.5% (n = 33)	5.7%
Dc14a13	14.4% (n = 154)	13.9%	5.7% (n = 25)	4.7%
Dc14a14	27.0% (n = 111)	20.5%	4.8% (n = 21)	4.3%
Dc14a15	16.6% (n = 134)	11.7%	6.9% (n = 13)	5.6%
Dc14a16	21.9% (n = 106)	14.7%	6.3% (n = 15)	4.5%
Dc14a17	24.6% (n = 145)	20.1%	9.2% (n = 35)	8.2%

cascade ablation [6] was used, which allows a controlled release of the fluid and possible daughter crystals. A transient signal for a fluid inclusion opened by a stepwise increase of the spot size is shown in Fig. 6. The variation of spot size can be followed with the Si signal, which represents the matrix (fluid inclusions hosted in quartz). Fluid-contained elements are observed in the early stages of the opening and the excellent time resolution of the TOFMS allows to detect afterwards very narrow transient peaks, e.g. Li, Cu, Zn, As and Sn, which are related to daughter crystals in the inclusions. These peaks occur after the ablation pit is enlarged enough for the crystal to escape from the inclusion (Fig. 6). In total 42 isotopes out of the list of 63 isotopes were detected. The analyte-to-sodium ratios were calculated for inclusions from the same trail, which are shown for a selection of isotopes in Fig. 7. These ratios were calculated based on the full integrals of the fluid inclusion (from the opening till the emptying). The fast signal recording allows distinguishing between elements contained in the fluid and elements contained in the crystal(s) in fluid inclusions by means of inter-element correlation. Figure 8 shows the example of correlated elements (^{85}Rb and ^{133}Cs versus ^{55}Mn), whereas ^{118}Sn is not correlated to any element determined in the fluid.

On the same natural inclusions the isotopic ratio precision for lead isotopes was determined in agreement with counting statistics [9]. Unfortunately, the modest sensitivity available so far limits the isotope ratio precision to 10% RSD for full signal ratios. In Table 4 the RSD of lead isotope ratios for the total signal and for the highest occurring peak are given. The improved RSD in single peak integration indicates that the quantification of the elemental composition in fluid inclusions and the determination of precise isotope ratios demand different ablation strategies. Therefore, where controlled sampling of elements is not so important as quantification, laser repetition rates above 10 Hz should be used to sample the inclusion in a shorter period of time with the best signal-to-noise ratio leading to improved isotope ratio precision.

Conclusions

ICP-time of flight mass spectrometry in combination with laser ablation can be the preferred technique for multielemental analysis of short transient signals. The optimized system offers a variety of interesting features for the application shown in this study. Especially the time resolution and the unlimited number of isotopes measurable are advantages for high spatial resolution analysis using laser ablation. Nevertheless, the modest sensitivity and the background level are currently limiting the applications of the ICP-TOFMS in solid sampling. The reduction of the ablation cell volume showed first improvements in sensitivity due to increased sample density in the plasma. However, further investigation of the transportation system including mixed gas studies will lead to a better understanding of the behavior of dry aerosols in the ICP-TOFMS.

Acknowledgements The authors are grateful to Mr. M. Küpfer and Mr. P. Steiner (Dept. of Chemistry, ETH Zurich) for the collaboration in the realization of the ablation cell. The project is supported by the ETH grant no. 0–11354–98.

References

1. Guilhaus M (1995) J Mass Spectrom 30: 1519–1532
2. Hieftje GM, Myers DP, Li G, Mahoney PP, Burgoyne TW, Ray SJ, Guzowski JP (1997) J Anal Atom Spectrom 12: 287–292
3. Vanhaecke F, Moens L, Dams R, Allen L, Georgitis S (1999) Anal Chem 71: 3297–3303
4. Tian X, Emteborg H, Adams FC (1999) J Anal Atom Spectrom 14: 1807–1814
5. Audetàt A (1999) Ph.D. dissertation ETH nr.13168
6. Günther D, Audetàt A, Frischknecht R, Heinrich CA (1998) J Anal Atom Spectrom 13: 263–270
7. Günther D, Frischknecht R, Heinrich CA, Kahlert HJ (1997) J Anal Atom Spectrom 12: 939–944
8. Emteborg H, Tian X, Adams FC (1999) J Anal Atom Spectrom 14: 1567–1572
9. Knoll GF (1999) Radiation detection and measurement. Wiley & Sons